Advanced Fiber Materials (2022) 4:246–255
https://doi.org/10.1007/s42765-021-00099-3

RESEARCH ARTICLE

Injectable Fiber Electronics for Tumor Treatment

Yang Zhao[1] · Chuanrui Chen[1] · Yangyang Qiu[2] · Tenglong Mei[1] · Lei Ye[1] · Huan Feng[2] · Ye Zhang[3] · Liyuan Wang[1] · Yue Guo[1] · Xuemei Sun[1] · Jiaxue Wu[2] · Huisheng Peng[1]

Received: 23 June 2021 / Accepted: 15 August 2021 / Published online: 13 September 2021
© Donghua University, Shanghai, China 2021

Abstract
Electrochemical therapy emerged as a low-cost and effective method for tumor ablation. However, it has challenges such as the production of toxic byproducts and the use of rigid electrodes that damage soft tissues. Here, we report a new injectable and tissue-compatible fiber therapeutic electronics for safe and efficient tumor treatment. The design of aligned carbon nanotube (CNT) fiber as electrodes endowed the device with high softness and enabled mini-invasive implantation through injection. Under a mild voltage (1.2 V), the fiber device released hydroxyl ions to alter the local chemical environment of the tissues without additional toxic products/gases, leading to immediate death of tumor cells. The flexible fiber device could form stable interface with tissues and showed good biocompatibility after implantation for 30 days. The in vitro experimental results showed the fiber device could efficiently kill 90.9% of QGY-7703 cancer cells after a single treatment in a few minutes. The tumor-bearing animal models proved that the fiber therapeutic device could effectively inhibit the growth of tumor tissues, indicating it is a safe, effective, controllable and low-cost method for tumor therapy.

Keywords Flexible · Biocompatible · Implantable · Fiber device · Tumor therapy

Introduction

The major clinical tumor treatment methods, including surgery, chemotherapy and radiotherapy, have been used as powerful tools to combat cancer for decades, although they have challenges such as high recurrence rate, toxicity and drug resistance [1–3]. Immunotherapy, gene therapy and nanomaterials mediated therapy have shown promises in tumor therapy [4–10]. However, there is still room to lower their cost and improve therapeutic efficiency [11–13]. On the other hand, flexible and miniaturized electronics is booming by designing new materials and structures for medical applications [14–17]. In particular, implantable electronics with photodynamic therapy and controlled drug release functions were developed for tumor therapy [18–21]. However, despite the success of these electronics, their therapeutic outcome is usually limited by the tumor site and pre-loaded drug amount, hence the development of a versatile and effective tumor treatment method is crucial [22–25].

Electrochemical therapy (EChT) appeared as a low-cost, effective and adaptable method for tumor ablation by utilizing a large direct current passing through metallic electrodes to induce the electrolysis reaction [26–28]. The reaction generates hydroxyl ions on the cathode to increase local pH to kill cancer cells. At the anode, oxygen evolution reaction causes an increase in acidity due to produced protons. However, the chlorine generated from the anode as a byproduct is toxic to normal tissues and causes long-term damage to normal tissues. Furthermore, traditional EChT uses rigid

Yang Zhao, Chuanrui Chen have contributed equally to the work.

✉ Xuemei Sun
sunxm@fudan.edu.cn

✉ Jiaxue Wu
jiaxue@fudan.edu.cn

✉ Huisheng Peng
penghs@fudan.edu.cn

[1] State Key Laboratory of Molecular Engineering of Polymers, Department of Macromolecular Science and Laboratory of Advanced Materials, Fudan University, Shanghai 200438, China

[2] The State Key Laboratory of Genetic Engineering, School of Life Science, Zhongshan Hospital, Fudan University, Shanghai 200438, China

[3] National Laboratory of Solid State Microstructures, Jiangsu Key Laboratory of Artificial Functional Materials, and College of Engineering and Applied Sciences, Nanjing University, Nanjing 210023, China

metallic electrodes like platinum and stainless steel, and the mechanical mismatch causes damages of soft tissues and adds extra discomfort and pain to patients [26, 27]. As a result, the problems such as toxic byproducts and the use of rigid electrodes have largely limited the progress and applications of EChT. It is critical to find mild, controllable and effective electrochemical reactions and flexible, biocompatible electrodes for safer and better EChT.

Here, we report a new kind of fiber devices for safe and efficient tumor treatment. Aligned carbon nanotube (CNT) fibers with both high electronic and mechanical properties were demonstrated as electrodes. The fiber device consists of a bare CNT fiber cathode and $Na_{0.44}MnO_2$ (NMO) particle-modified CNT fiber anode, and the operation voltage was only 1.2 V, lower than the theoretical water hydrolysis potential window. The therapeutic fiber device is flexible and biocompatible, and could be mini-invasively injected into the specific tumor site. The cathode fiber could rapidly and accurately release hydroxyl ions (OH^-) via oxygen reduction reaction (ORR), and the rapid change of the local chemical environment is harsh for cancer cells to survive, thus leading to the lysis and death of tumor cells and tumor growth inhibition. The NMO particle-modified anode fiber could complete the circuit through controllable electrochemical reactions, without additional toxic chemicals/gases generated during the treatment process to avoid side effects on normal tissues. Furthermore, the high flexibility of the CNT fiber electrode offered high tissue compatibility during implantation for 30 days. The tumor-bearing animal model showed the fiber therapeutic device inhibited the average tumor volume under 34 mm^3 on the 9th day, while the tumor volume in the control group was close to 300 mm^3. Compared with the existing EChT, the new therapeutic device based on fiber electronics is safer, effective and controllable.

Experimental Section

Preparation of Fiber Cathode and Anode

The CNT fiber as the cathode was synthesized via floating catalyst chemical vapor deposition method. To prepare the CNT/NMO fiber anode, NMO particles were synthesized by mixing Na_2CO_3 and Mn_3O_4 at molar ratio of 0.726:1. The mixture was grinded for 30 min and then heated in a muffle furnace at 500 °C for 5 h, with a temperature increasing rate of 5 °C/min. The Resulting sample was further grinded for 15 min and heated in a furnace at 900 °C for 10 h. The NMO powders were collected and dispersed in ethanol. At the same time, aligned CNT sheet was dry-drawn from spinnable CNT array, and the NMO dispersion was finally added to the CNT sheet, followed by twisting through a rotor to produce the CNT/NMO fiber anode.

Electrochemical Characterization of Fiber Device

Oxygen reduction reaction of fiber cathode was tested on electrochemical working station (Shanghai Chenhua, CHI660e). A typical three electrode configuration was used for the test. The 0.1 M phosphate-buffered saline as test medium was purged with N_2 or O_2 for 30 min before testing. Cyclic voltammetry was made in electrochemical window between − 1.0 and 0 V with scan speed of 100 mV/s. The linear sweep voltammetry was scanned from 0 to − 1.0 V with a scan speed of 100 mV/s. The simulations were performed by using the transient diffusion modules of COMSOL Multiphysics software. To simulate the longitudinal and cross-sectional release of chemicals from fiber cathode, the simulation models were built up by placing a fiber electrode with diameter of 10 μm in the middle of 1 cm^2 square space which was filled with water. The diffusion coefficient of hydroxide ions in water is 5.27×10^{-5} cm^2/s.

Biocompatibility Study

First, L929 fibroblasts were cultured on glass substrate (control group) and with CNT fiber electrode (experimental group). After 5 days, the cells at both groups were stained with Cellbrite Red and Nuclear Blue DCS1 and observed under confocal microscope. Mice were randomly divided into control and experimental groups. For the control group, no fiber device was injected. For the experimental group, the fiber device was injected into the hind leg. Two groups of mice were cultured for 30 days before sacrificed. The muscle tissues were dissected and fixed with 4% paraformaldehyde for 5 h. The tissue samples were gradually dehydrated in ethanol and then stained with H&E, F4/80 and LY-6G. The samples were observed under a microscope. To study the toxicity of fiber device, the heart, liver, spleen, lung and kidney from the control and experimental groups were dissected and fixed with 4% paraformaldehyde for 24 h. The samples were then dehydrated in ethanol before H&E staining.

In Vitro Assessment of Therapeutic Effect

QGY-7703 cells were used to verify therapeutic effect of fiber device in vitro. The cell culture media was replaced to saline before testing, and fiber cathode and anode were incubated in the solution. Then a voltage of 1.2 V was applied on the fiber device by using an electrochemical station, and the charge quantity was controlled between 0 and 0.02 C. The cell morphology was observed under an optical microscope. The therapeutic effect of fiber device on the colony of QGY-7703 cells was tested similarly.

In Vivo Study of Therapeutic Effect

All animal experiments were conducted under a protocol approved by the Animal Experimentation Committee of Fudan University. To construct the tumor-bearing animal model, QGY-7703 cells were injected in the subcutaneous area of nude mice. The mice were then randomly divided into control and experimental groups. Fiber device was injected into the tumor via a syringe. The mice in the control group were implanted with fiber device but without electrochemical treatment. The mice in the experimental group were treated by applying 1.2 V voltage on fiber device for 10 min every day. Since the beginning of the treatment, the sizes of the tumor were measured every day with a vernier caliper. The tumor volume (V) was calculated from the following equation: $V = \text{width}^2 \times \text{length}/2$. The tumors were dissected and stained with H&E, Ki-67 and Caspase 3 for further study.

Results and Discussion

Figure 1a shows the implantation process of the injectable fiber device. Due to the small size, it could be injected into the tumor site through a mini-invasive syringe. The fiber device consisted of two electrodes, namely bare CNT fiber as cathode and CNT/NMO hybrid fiber as anode. With the use of low operating voltage of 1.2 V, the cathode initiated ORR to generate hydroxyl ions, while NMO particles in the anode released harmless sodium ions to complete the full electrochemical reaction with cathode (Fig. 1b). The released hydroxyl ions changed the local pH to alkaline to

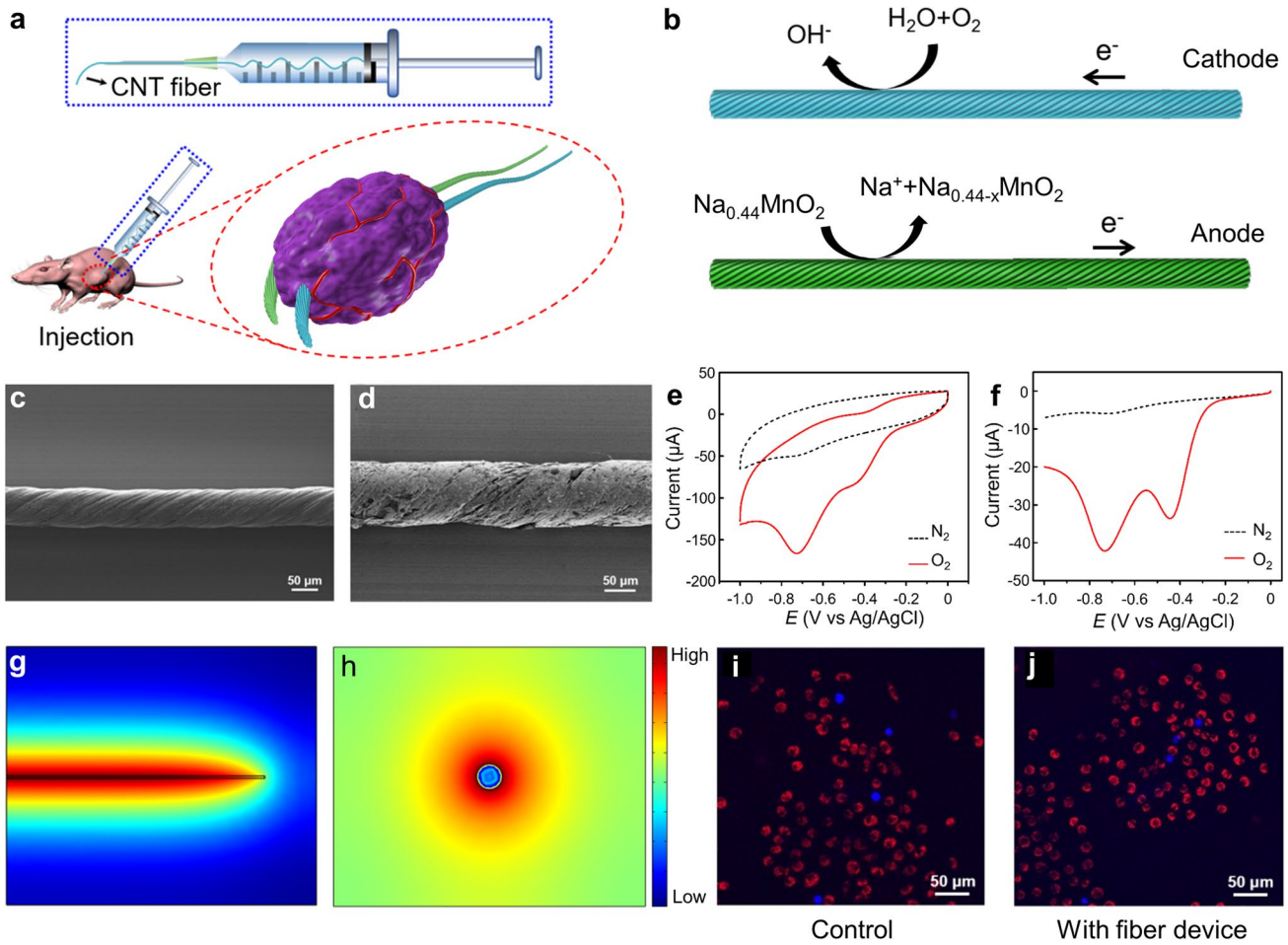

Fig. 1 Working mechanism, structure characterization, electrochemical property and cell compatibility of the injectable tumor-therapeutic fiber device. **a** Scheme illustrating the injecting process of fiber device into a tumor. **b** Working mechanism of fiber device. ORR on the cathode causes the release of hydroxyl ions. **c**, **d** SEM images of fiber cathode and anode, respectively. **e**, **f** Cyclic voltammetry and linear sweep voltammetry of fiber cathode in the presence and absence of O_2, respectively. **g**, **h** The simulated longitudinal (**g**) and cross-sectional (**h**) models showing the homogeneous release of chemicals from fiber cathode. **i**, **j** Confocal images of L929 cells cultured without and with fiber device for 5 days, respectively. Blue: Nuclear Blue DCS1 stained dead cells; red: Cellbrite Red stained living cells

create highly toxic environment for tumor cells, thus leading to immediate death of tumor cells in minutes. NMO particles were chosen as active material for anode because they can complete the circuit without generating additional toxic chemicals/gases to prevent the damage to normal tissues. The electrochemical reactions on the two fiber electrodes are demonstrated as follow:

$$O_2 + 2H_2O + 4e^- \rightarrow 4OH^-$$

$$Na_{0.44}MnO_2 - xe^- \rightarrow Na_{0.44-x}MnO_2 + xNa^+$$

The cathode was based on bare aligned CNT fiber with diameter of ~ 75 μm (Fig. 1c) with aligned channels typically ranged from tens to hundreds of nanometers inside (Fig. S1), which was beneficial for the infiltration of body fluids and subsequent ORR. The CNT fiber cathode was flexible and robust, and it can be tied into a knot without breaking (Fig. S2). NMO nanoparticles were wrapped into aligned CNTs to produce the hybrid anode (Figs. 1d and S3). To study the electrocatalytic oxygen reduction behavior of the fiber cathode, cyclic voltammetry and linear sweep voltammetry of the cathode in the presence and absence of O_2 was compared (Fig. 1e, f). Two reduction peaks at − 0.44 and − 0.73 V indicated the cathode went through two successive two-electron reaction processes, while no peak was observed in N_2 purged media, proving the occurrence of ORR on the cathode [29].

The linear sweep voltammetry further showed the detailed ORR performance of the cathode in oxygen-rich and anaerobic environment. The reduction peaks were more distinguishable in oxygen-rich environment due to suppressed non-faradic current, while a plateau appeared when the voltage was scanned from 0 to − 1 V in N_2 purged PBS buffer. The reduction current showed a sharp decrease at − 0.2 V due to the start of ORR reaction in oxygen-rich environment, and the cathode current peaked at − 0.73 V, showing the reaction reached the diffusion control region. To ensure a rapid and sufficient OH^- release rate, the operation voltage of the fiber therapeutic device was set at 1.2 V, which was below the theoretical decomposition voltage of water (1.23 V). Modeling was performed to demonstrate the chemical gradient built up around the electrode (Fig. 1g, h), thus visualizing the 'killing zone' for tumor cells, which was established by the released hydroxide ions from the cathode.

Implantable electronic devices directly contacted human tissues, and it is important to guarantee their safety to avoid foreigner-body response and immune rejection [16, 30]. We have carefully investigated the biocompatibility of the fiber therapeutic device. First, we traced its cytotoxicity through cell experiments. L929 fibroblasts were cultured on glass substrate (control group) and with CNT fiber electrode (experimental group). After 5 days, the cells at both groups were stained to identify live/dead cells. As shown in Fig. 1i, j, no significant differences were found in the survival rate and morphology of the cells between experimental and control groups, indicating that the fiber device showed no obvious cytotoxicity.

The mechanical matching between implantable devices and soft tissue is a crucial factor for the tissue compatibility of the device [30, 31], thus the biocompatibility of the fiber device is evaluated, as demonstrated in Fig. 2. Aligned CNT fiber had low bending stiffness and is mechanically compatible with soft tissue, and they thus could form stable device-tissue interface, so it is an ideal electrode for implantable devices [32]. To further confirm the bio-safety of the fiber device, we systemically study the tissue compatibility on the mouse model. A group of mice was randomly divided into experimental (with implants) and control groups (without implants), and the muscle tissue was stained with H&E dyes after 30 days. As shown in Fig. 2a, b, the muscle tissue around the implanted device site did not undergo significant changes in terms of tissue morphology, indicating the fiber device was compatible and formed a stable interface with the muscle tissue.

In addition, we performed immunofluorescence staining for F4/80 and LY-6G antibodies on the experimental and control groups to study the immune cell reactions after implantation. As shown in Fig. 2c–f, no significant difference between the F4/80 and LY-6G positive cells was identified between the control and experimental groups. Therefore, the implanted fiber device caused almost negligible infiltration for macrophages and neutrophils with high biocompatibility. We further analyzed the main organs (e.g., heart, liver, spleen, lung and kidney) of the mouse by pathological H&E staining after 30 days of implantation to verify whether the fiber device caused systemic pathological toxicity (Fig. 2g). Compared with the control group, the main organs in the experimental group did not show obvious pathology change or tissue damage. After the fiber device was implanted for 30 days, no obvious systematic side effects and safety concerns were produced.

The therapeutic effect of the fiber device in vitro was then tested in saline, and the medium pH effectively changed to alkaline after treated with different quantities of electric charge (Fig. 3a). With a phenolphthalein-loaded agar gel, we could clearly visualize the OH^- generation and diffusion caused by the fiber device (Fig. S4). Further, we used the fiber device to treat human hepatoma carcinoma QGY-7703 cells with different electric quantities. The change of cell morphology of QGY-7703 tumor cells over time after treated with a certain electric quantity by the fiber device was investigated in Fig. 3b–d. The QGY-7703 cells maintained spindle shape and adherent form at 0 s, while after treatment for 720 s, most tumor cells were completely lysed. Therefore, the microenvironment can be

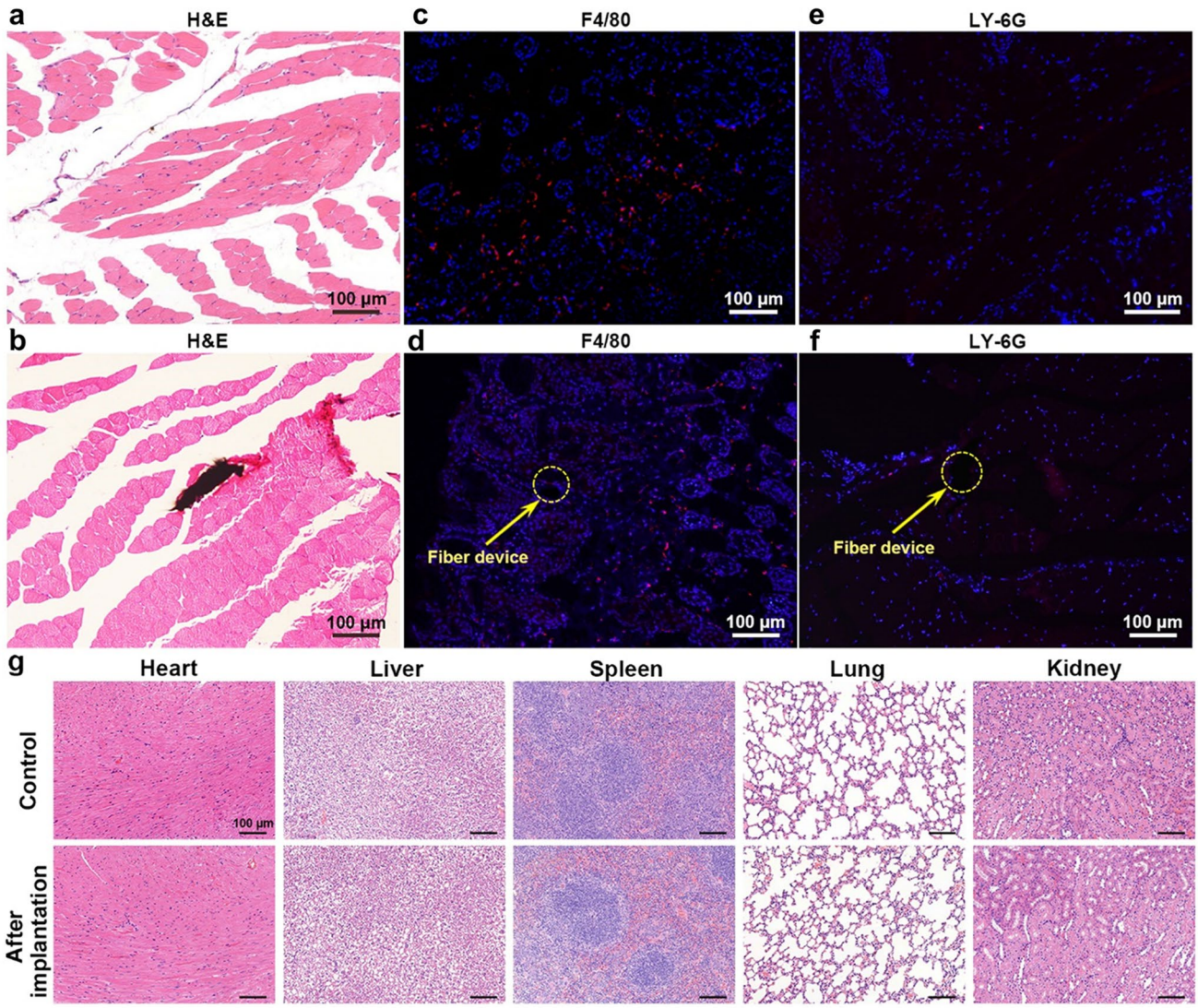

Fig. 2 Biocompatibility study of the injectable fiber device. **a**, **b** Hematoxylin and eosin (H&E) stained images of control group and experiment group for 30 days in mouse muscle tissues, respectively. **c**, **d** F4/80 immunofluorescence staining (marker for macrophages) of control and experimental groups, respectively. Blue and red fluorescence indicate cell nucleus and F4/80 antibody expression, respectively. **e**, **f** LY-6G immunofluorescence staining (marker for neutrophils) of control and experimental groups, respectively. Blue and red fluorescence indicate cell nucleus and LY-6G antibody expression, respectively. **g** Pathological H&E section staining images of major organs (heart, liver, spleen, lung and kidney) in control and experimental groups after implanting fiber devices for 30 days

changed by the fiber device to promote the lysis and death of tumor cells.

We have further investigated the survival rate of tumor cells upon treated with different electric quantities by the fiber device (Fig. 3e). After treatment with Q/3 and Q electric charges (Q = 0.02 C), the survival rates of QGY-7703 tumor cells were reduced to 15.3% and 9.1%, respectively. Therefore, the fiber device showed an obvious killing effect on QGY-7703 tumor cells, and the effect was enhanced with the increasing treatment electric quantity. In addition, the clone formation rate experiment was carried out to further study the influence of fiber device on the killing effect of tumor cells (Fig. 3f–h). With the increasing treatment charge quantities, the clone of the QGY-7703 was destroyed and the killing effect was enhanced (up to 0.02 C). Therefore, the fiber device had rapid and efficient killing effect on tumor cells, and the therapeutic outcome can be effectively adjusted by varying the electric charge quantity.

To test the tumor-killing effect of the fiber device in vivo, QGY-7703 tumor cells were injected into the subcutaneous tissues of nude mice to construct the animal model (Fig. 4). The tumor-bearing mice were then divided into control and experimental group. Fiber devices were implanted and applied voltage in the experimental group, while fiber

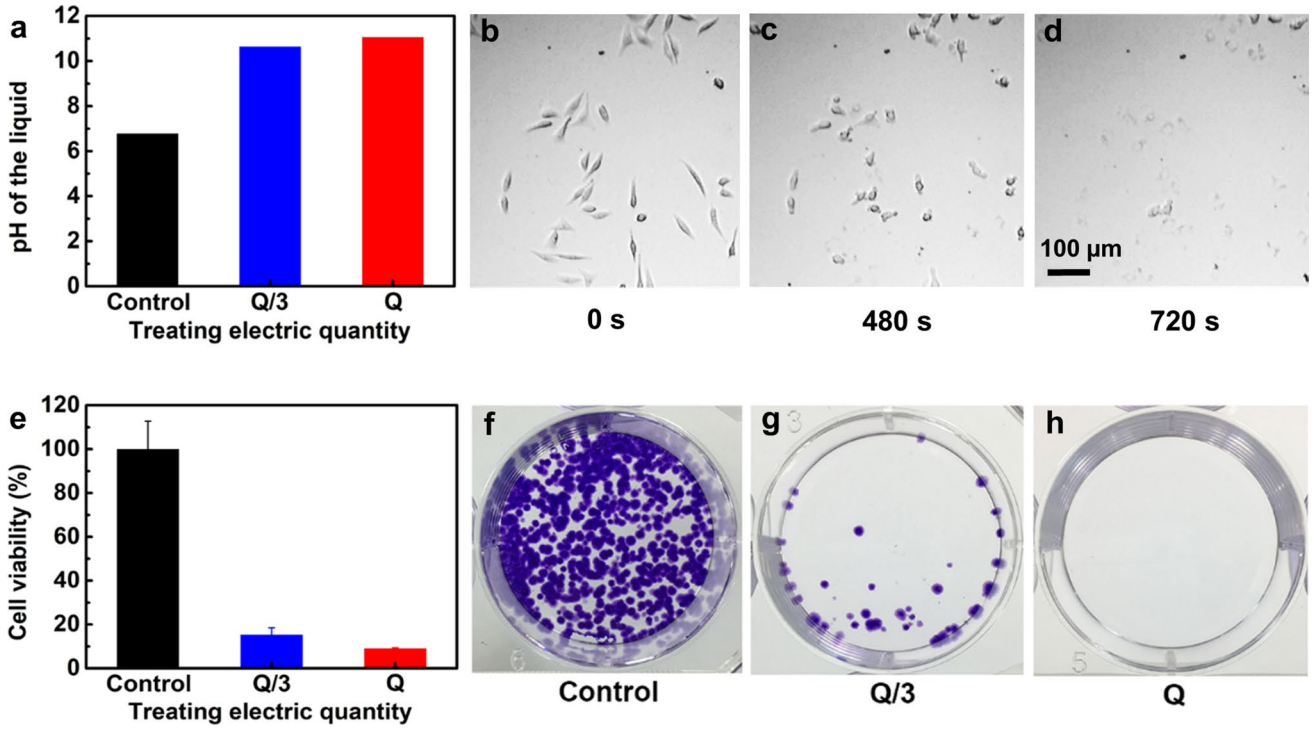

Fig. 3 In vitro assessments of therapeutic effect of injectable fiber device. **a** The pH-regulating effect of the injectable fiber device with different treating electric quantities (Q = 0.02 C). **b–d** Representative microscopic images of QGY-7703 tumor cells at 0, 480 and 720 s with the treatment of fiber device, respectively. **e** Tumor cell viability after the treatment of different electric quantities. **f–h** The colony of QGY-7703 cells treated by fiber devices with different electric quantities

devices were implanted but without electrical treatment in the control group. As shown in Fig. 4a, b, the tumor sizes in the experimental group became significantly smaller. In contrast, the sizes of the tumors in the control group have grown much larger. We have measured the change of tumor volume in the experimental and control groups over time (Fig. 4c). The tumor volume in the experimental group started to decrease after the device treatment and then remained relatively stable, demonstrating the tumor growth had been successfully suppressed. On the other hand, the tumor tissues in the control group grew rapidly. The average tumor volume in the control group was close to 300 mm^3 on the 9th day, while the average tumor volume of nude mice was under 34 mm^3 in the experimental group. The above results proved the fiber device had effective inhibitory effect on the growth of tumor tissues.

We further performed H&E staining on the tumor tissues in the experimental and control groups after the treatment (Fig. 4d). The staining image in the control group showed the cells in the tumor tissue were tightly arranged at a normal and rapid proliferation state. As a comparison, the density of tumor cells had been greatly reduced after the treatment of fiber device; the residue cells shared an abnormal morphology, showing the treatment has largely damaged the tumor tissue. Later, immunofluorescence analyses of Ki-67 (indicator for cell proliferation) and Caspase 3 (indicator for cell apoptosis) antibodies were conducted to further study the treatment effect on tumor cells. The fluorescent staining images showed that there was a large amount of Ki-67 antibody expression and almost no obvious Caspase 3 expression in the control group (without treatment of fiber device), indicating the tumor cells were at rapid proliferation state [33]. On the contrary, there was almost no obvious expression of Ki-67 antibody in the experimental group, proving the proliferation of tumor cells had been greatly suppressed [34]. In addition, the Caspase 3 immunofluorescence staining image in the experimental group showed most cells were at an apoptotic state. It is thus concluded that the fiber device can effectively suppress tumor growth by inhibiting the proliferation and promoting the apoptosis of tumor cells.

Conclusions

In summary, a systematical study on the safety and tumor-killing effect of the fiber therapeutic device has been conducted on cellular, tissue and animal model levels. Thanks to its high softness and biocompatible CNT fiber electrode with mild, controllable electrochemical reaction, the fiber device can be mini-invasively injected into the

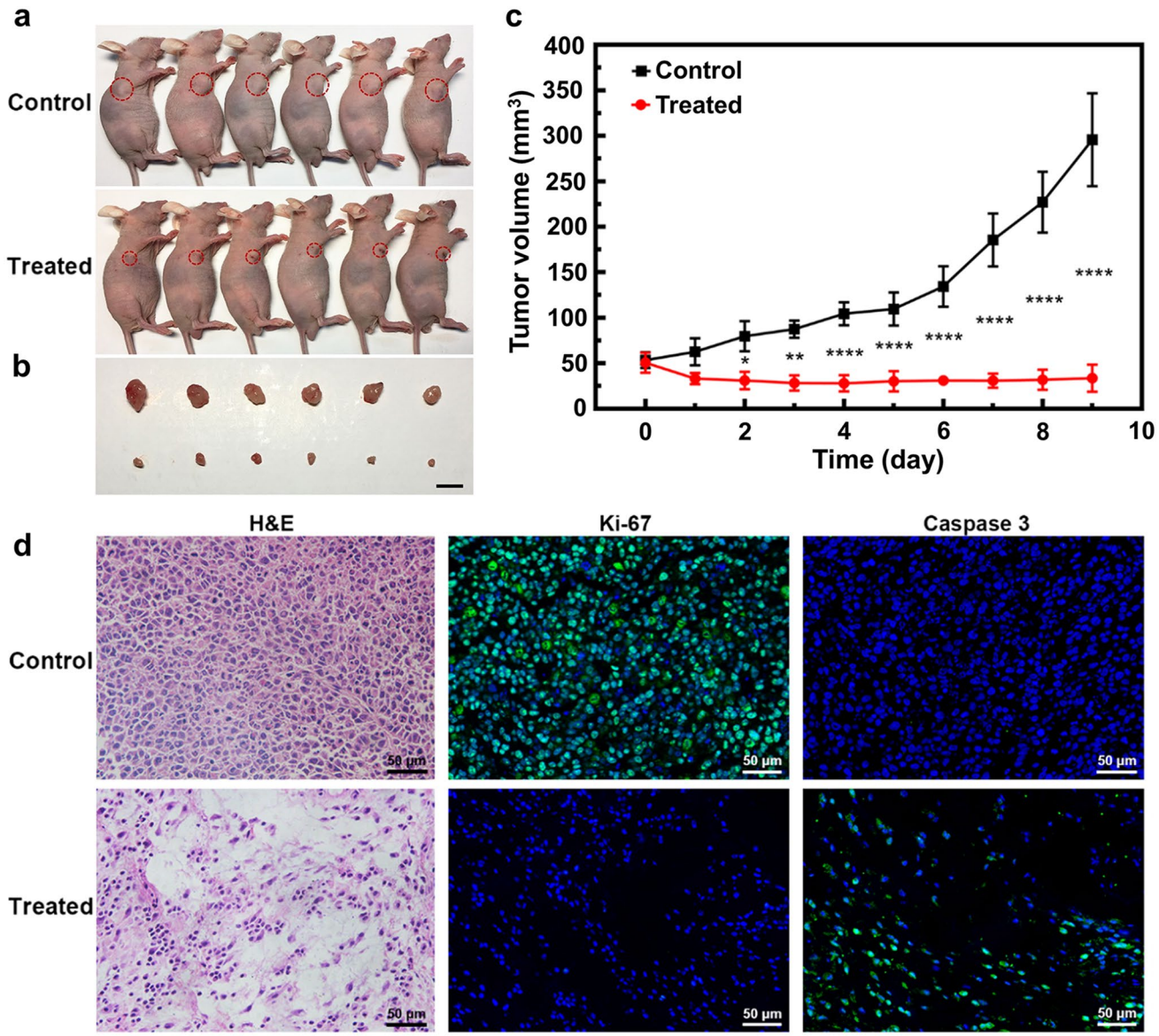

Fig. 4 In vivo tumor-killing effect of fiber device. **a** Photographs of mice without and with the treatment of fiber device after 9 days. The red dotted lines indicate the tumor locations. **b** Photographs of the tumor tissues from the mice without and with the treatment of fiber device after 9 days. Scale bar, 1 cm. **c** Changes in the tumor volumes of nude mice inoculated with QGY-7703 cells over time. **d** H&E staining, Ki-67 (indicator for cell proliferation) and Caspase 3 (indicator for cell apoptosis) immunofluorescence analysis of the tumor tissues without and with the treatment of fiber device. The nucleus is shown in blue (DAPI) while Ki-67 and Caspase 3 are shown in green

specific tumor site and achieve safe and effective tumor treatment. The tumor-bearing animal models have proved that the fiber therapeutic device could effectively inhibit the growth of tumor tissues. Compared to traditional EChT using rigid metal electrodes, tissue-compatible fiber devices did not produce additional toxic components during tumor treatment, indicating it is a safe, effective, controllable and low-cost method for tumor therapy. This work may present a new and effective route in the development of fiber electronics for biomedical applications such as disease diagnosis and treatment in the future.

Supplementary Information The online version contains supplementary material available at https://doi.org/10.1007/s42765-021-00099-3.

Acknowledgements This work was supported by MOST (2016YFA0203302), NSFC (21634003, 22075050), STCSM (20JC1414902), SHMEC (2017-01-07-00-07-E00062), the National Postdoctoral Program for Innovative Talents (BX2021245) and the Fundamental Research Funds for the Central Universities.

Declarations

Conflicts of interest There are no conflicts to declare.

References

1. Gatenby RA, Brown JS. Integrating evolutionary dynamics into cancer therapy. *Nat Rev Clin Oncol*. **2020**;*17*:675.
2. Moeller BJ, Richardson RA, Dewhirst MW. Hypoxia and radiotherapy: opportunities for improved outcomes in cancer treatment. *Cancer Metastasis Rev*. **2007**;*26*:241.
3. Vaupel P, Thews O, Hoeckel M. Treatment resistance of solid tumors. *Med Oncol*. **2001**;*18*:243.
4. Lesterhuis WJ, Haanen JB, Punt CJ. Cancer immunotherapy-revisited. *Nat Rev Drug Discov*. **2011**;*10*:591.
5. Huo M, Wang L, Wang Y, Chen Y, Shi J. Nanocatalytic tumor therapy by single-atom catalysts. *ACS Nano*. **2019**;*13*:2643.
6. Zhou Z, Liu X, Zhu D, Wang Y, Zhang Z, Zhou X, Qiu N, Chen X, Shen Y. Nonviral cancer gene therapy: delivery cascade and vector nanoproperty integration. *Adv Drug Deliv Rev*. **2017**;*115*:115.
7. Musetti S, Huang L. Nanoparticle-mediated remodeling of the tumor microenvironment to enhance immunotherapy. *ACS Nano*. **2018**;*12:*11740.
8. Barreto JA, O'Malley W, Kubeil M, Graham B, Stephan H, Spiccia L. Nanomaterials: applications in cancer imaging and therapy. *Adv Mater*. **2011**;*23*:H18.
9. Wang SB, Zhang C, Chen ZX, Ye JJ, Peng SY, Rong L, Liu CJ, Zhang XZ. A versatile carbon monoxide nanogenerator for enhanced tumor therapy and anti-inflammation. *ACS Nano*. **2019**;*13*:5523.
10. Chen W, Du J. Ultrasound and pH dually responsive polymer vesicles for anticancer drug delivery. *Sci Rep*. **2013**;*3*:2162.
11. Li Z, Chen L, Rubinstein MP. Cancer immunotherapy: are we there yet? *Exp Hematol Oncol*. **2013**;*2*:1.
12. Restifo NP, Smyth MJ, Snyder A. Acquired resistance to immunotherapy and future challenges. *Nat Rev Cancer*. **2016**;*16*:121.
13. Björnmalm M, Thurecht KJ, Michael M, Scott AM, Caruso F. Bridging bio-nano science and cancer nanomedicine. *ACS Nano*. **2017**;*11*:9594.
14. Zhong J, Zhong Q, Hu Q, Wu N, Li W, Wang B, Hu B, Zhou J. Stretchable self-powered fiber-based strain sensor. *Adv Funct Mater*. **2015**;*25*:1798.
15. Xiao F, Li Y, Zan X, Liao K, Xu R, Duan H. Growth of metal-metal oxide nanostructures on freestanding graphene paper for flexible biosensors. *Adv Funct Mater*. **2012**;*22*:2487.
16. Cai P, Leow WR, Wang X, Wu YL, Chen X. Programmable nano-bio interfaces for functional biointegrated devices. *Adv Mater*. **2017**;*29*:1605529.
17. Wang Y, Chen C, Xie H, Gao T, Yao Y, Pastel G, Han X, Li Y, Zhao J, Fu K. 3D-printed all-fiber li-ion battery toward wearable energy storage. *Adv Funct Mater*. **2017**;*27*:1703140.
18. Zhao C, Feng H, Zhang L, Li Z, Zou Y, Tan P, Ouyang H, Jiang D, Yu M, Wang C. Highly efficient in vivo cancer therapy by an implantable magnet triboelectric nanogenerator. *Adv Funct Mater*. **2019**;*29*:1808640.
19. Li B, Ji P, Peng SY, Pan P, Zheng DW, Li CX, Sun YX, Zhang XZ. Nitric oxide release device for remote-controlled cancer therapy by wireless charging. *Adv Mater*. **2020**;*32*:2000376.
20. Bansal A, Yang F, Xi T, Zhang Y, Ho JS. In vivo wireless photonic photodynamic therapy. *Proc Natl Acad Sci*. **2018**;*115*:1469.
21. Yamagishi K, Kirino I, Takahashi I, Amano H, Takeoka S, Morimoto Y, Fujie T. Tissue-adhesive wirelessly powered optoelectronic device for metronomic photodynamic cancer therapy. *Nat Biomed Eng*. **2019**;*3*:27.
22. Chew SA, Danti S. Biomaterial-based implantable devices for cancer therapy. *Adv Healthc Mater*. **2017**;*6*:1600766.
23. Wang X, Lv F, Li T, Han Y, Yi Z, Liu M, Chang J, Wu C. Electrospun micropatterned nanocomposites incorporated with Cu_2S nanoflowers for skin tumor therapy and wound healing. *ACS Nano*. **2017**;*11*:11337.
24. Talebian S, Foroughi J, Wade SJ, Vine KL, Dolatshahi-Pirouz A, Mehrali M, Conde J, Wallace GG. Biopolymers for antitumor implantable drug delivery systems: recent advances and future outlook. *Adv Mater*. **2018**;*30*:1706665.
25. Zhang L, Wang Z, Zhang Y, Cao F, Dong K, Ren J, Qu X. Erythrocyte membrane cloaked metal-organic framework nanoparticle as biomimetic nanoreactor for starvation-activated colon cancer therapy. *ACS Nano*. **2018**;*12*:10201.
26. Nilsson E, Euler H, Berendson J, Thörne A, Wersäll P, Näslund I, Lagerstedt AS, Narfström K, Olsson JM. Electrochemical treatment of tumours. *Bioelectrochemistry*. **2000**;*51*:1.
27. Cury FL, Bhindi B, Rocha J, Scarlata E, Jurdi KE, Ladouceur M, Beauregard S, Vijh AK, Taguchi Y, Chevalier S. Electrochemical red-ox therapy of prostate cancer in nude mice. *Bioelectrochemistry*. **2015**;*104*:1.
28. Gu T, Wang Y, Lu Y, Cheng L, Feng L, Zhang H, Li X, Han G, Liu Z. Platinum nanoparticles to enable electrodynamic therapy for effective cancer treatment. *Adv Mater*. **2019**;*31*:1806803.
29. Wiggins-Camacho JD, Stevenson KJ. Mechanistic discussion of the oxygen reduction reaction at nitrogen-doped carbon nanotubes. *J Phys Chem C*. **2011**;*115*:20002.
30. Feiner R, Dvir T. Tissue-electronics interfaces: from implantable devices to engineered tissues. *Nat Rev Mater*. **2017**;*3*:1.
31. Xu X, Xie S, Zhang Y, Peng H. The rise of fiber electronics. *Angew Chem Int Ed*. **2019**;*58*:13643.
32. Wang L, Xie S, Wang Z, Liu F, Yang Y, Tang C, Wu X, Liu P, Li Y, Saiyin H, Zheng S, Sun X, Xu F, Yu H, Peng H. Functionalized helical fibre bundles of carbon nanotubes as electrochemical sensors for long-term in vivo monitoring of multiple disease biomarkers. *Nat Biomed Eng*. **2020**;*4*:159.
33. Porter AG, Jänicke RU. Emerging roles of caspase-3 in apoptosis. *Cell Death Differ*. **1999**;*6*:99.
34. Scholzen T, Gerdes J. The Ki-67 protein: from the known and the unknown. *J Cell Physiol*. **2000**;*182*:311.

Yang Zhao is currently an associate professor in Northwestern Polytechnical University. He received his Ph.D. degree in Macromolecular Chemistry and Physics from Fudan University in 2020. His research interests are focused on the development of flexible and multi-functional energy storage devices with high safety.

Chuanrui Chen is a postdoctoral researcher at Fudan University in Prof. Huisheng Peng's group. His research interests include electrochemistry and biosensors. He received his Ph.D. degree at Wuhan University of Technology in 2018.

Huan Feng obtained her master's degree in 2020 from Fudan University. Her research mainly focuses on the molecular mechanism and treatment of liver cancer .

Yangyang Qiu obtained his master's degree in 2019 from Fudan University. His research mainly focuses on the molecular mechanism and treatment of liver cancer.

Ye Zhang is currently an associate professor at the College of Engineering and Applied Sciences at the Nanjing University. She received her Ph.D. degree in Macromolecular Chemistry and Physics from the Fudan University in 2018 and then joined the Harvard Medical School as a postdoctoral research fellow. Her research focuses on the development of soft electronics including batteries, sensors, and bioelectronic devices.

Tenglong Mei received his master's degree in 2021 from Fudan University. His research interest focuses on the biodegradable and rechargeable fiber battery.

Liyuan Wang received her Ph.D. degree from Fudan University in 2021. Now, she is a postdoctoral researcher in Department of macromolecular science, Fudan University. Her research interests focus on the application of the implantable fiber device in vivo.

Lei Ye received her B.S. degree at Sichuan University in 2017. She is currently a Ph.D. candidate of Laboratory of Advanced Materials, Fudan University. Her research interests include carbon materials and their applications in rechargeable alkali metal batteries.

Yue Guo obtained her bachelor's degree in 2019 from Central South University. She is currently a master student in Fudan University under the supervision of Prof. Huisheng Peng. Her research mainly focuses on fiber-based electrochemical sensor and biofuel cells.

Xuemei Sun received her Ph.D. in 2013 from Fudan University. Since 2018, she is an associate professor at Fudan University. Her research centers on flexible and implantable fiber materials and devices.

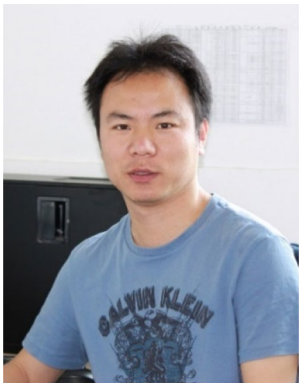

Jiaxue Wu obtained his Ph.D. in 2006 from Fudan University. Since 2011, he is a full professor in Fudan University. His main research focuses on the molecular mechanism of tumor development.

Huisheng Peng is currently Changjiang Chair Professor at Department of Macromolecular Science and Laboratory of Advanced Materials at Fudan University. He received his B.S. in Polymer Materials at Donghua University in China in 1999, M.S. in Macromolecular Chemistry and Physics at Fudan University in China in 2003 and Ph.D. in Chemical Engineering at Tulane University in USA in 2006. He then worked at Los Alamos National Laboratory before joining Fudan University in 2008. He starts and centers on the new direction of fiber electronics.